JOURNAL OF Materials CHEMISTRY

High temperature ceramics for use in membrane reactors: the development of microporosity during the pyrolysis of polycarbosilanes

Howard M. Williams,[a] Elizabeth A. Dawson,[a] Philip A. Barnes,*[a] Brian Rand,[b] Rik M. D. Brydson[b] and Adrian R. Brough[b]

[a]*Centre for Applied Catalysis, Materials Research Division, Department of Chemical and Biological Sciences, University of Huddersfield, Queensgate, Huddersfield, UK HD1 3DH*
[b]*Department of Materials, School of Process, Environmental and Materials Engineering, University of Leeds, Leeds, UK LS2 9ST*

Received 19th June 2002, Accepted 24th September 2002
First published as an Advance Article on the web 10th October 2002

The pyrolysis of polycarbosilane (PCS), a ceramic precursor polymer, at temperatures up to 700 °C under an inert atmosphere results in the development of amorphous microporous materials which have a number of potential applications, such as gas separation membranes. This paper investigates the development of microporosity during pyrolysis under nitrogen, at temperatures ranging from 300 to 700 °C, of both the cross-linked and non-cross-linked starting materials. The products are characterised by nitrogen adsorption, to determine surface areas and pore volumes, solid-state NMR, electron microscopy and FTIR, and their formation is studied using thermal analysis and evolved gas analysis with on-line mass spectrometry. The cross-linked and non-cross-linked PCSs have a maximum micropore volume of 0.2 $cm^3\ g^{-1}$ at pyrolysis temperatures of between 550 and 600 °C. The microporosity is stable in air at room temperature, but is lost in oxidising atmospheres at elevated temperatures.

1 Introduction

Ceramic precursor materials, such as polycarbosilanes, have been used for the preparation of ceramic fibres,[1,2] ceramic coatings[3] and SiC preforms.[4] While the pyrolysis of these materials has been extensively investigated,[5–7] the development of microporosity during the initial stages of pyrolysis has received less attention. The microporosity starts to develop at pyrolysis temperatures above 300 °C but, we found, is lost at temperatures above 700 °C.

Li and co-workers[8–10] used the microporosity developed during pyrolysis to 750 °C to produce inorganic microporous membranes for gas separation at high temperature. Shelekhin *et al.*[11] and Grosgogeat *et al.*[12] reported similar gas separation membranes manufactured *via* the pyrolysis of polysilastyrene. The development of microporosity in a range of ceramic precursor materials was investigated by Dismukes and co-workers,[13,14] who suggested that they could be used either as materials which show better thermal shock resistance in reducing atmospheres than microporous oxide materials, or for dielectric applications.

Our interest in these materials arises from the need for new inorganic membrane reactor[15] systems. Such reactors combine reaction and selective separation in one unit, with the separation stage occurring across the porous membrane. Reactions suitable for this type of reactor include dehydrogenations, which are equilibrium limited, where hydrogen is removed selectively across the membrane. Most current membrane reactors use γ-alumina to effect separation, but there are several problems with this material,[16] including the difficulty of manufacturing pores of sufficiently small diameter and its lack of stability at high temperatures. There is a clear requirement for membrane materials that have a suitable pore structure which is maintained at elevated temperatures.

The pyrolysis of polycarbosilanes occurs in a series of stages,[6] the first of which (to 550 °C) involves the evaporation of low molecular weight components with no apparent structural changes in the material. The next stage (to 850 °C) occurs with the evolution of methane and hydrogen, and is accompanied by structural changes in the material as it develops an amorphous inorganic structure. Finally, the β-SiC phase starts to develop at pyrolysis temperatures above 1100 °C. The exact mechanisms and temperatures depend on the method used to produce the PCS starting material.

A number of different routes can be used to prepare polycarbosilanes. These include heating polydimethylsilane in an autoclave at 470 °C for 14 h,[17] the thermal decomposition and condensation of tetramethylsilane at 770 °C[18] and refluxing polydimethylsilane with polyborodiphenylsiloxane (PBDPSO) under nitrogen at 350 °C.[19] The last method is attractive as it can be carried out easily at atmospheric pressure and relatively low temperatures, but it has been reported[20] that the PCS produced by this method, sometimes denoted PC-B in the literature, has fewer Si–H and more Si–Si bonds than PCS prepared by the other methods.

Some uses of polycarbosilane require curing or cross-linking of the material, such as in the production of fibres,[21] where the spun fibres are cured as the non-cross-linked material melts on pyrolysis. This involves heating in air at 200 °C to develop Si–O–Si bonds, a process which is accompanied by a weight gain. The resulting cross-linked material, which may be compared to a thermoset polymer, is insoluble. The cross-linking process adds oxygen to the system and has been shown[5] both to increase the temperature at which β-SiC crystallites start to form and to reduce crystal growth.

Microporosity is also seen in activated carbons. Carbons, from a wide variety of sources, can be prepared thermally in a two-stage process where a char is formed by heating a carbon precursor material in an inert atmosphere, followed by activation at temperatures of 800 to 1000 °C in an oxidising atmosphere of steam or CO_2. This leads to amorphous, microporous materials with large pore volumes, typically in excess of 0.3 $cm^3\ g^{-1}$, and surface areas greater than 500 $m^2\ g^{-1}$. The first stage produces a carbon-rich material, while the

 DOI: 10.1039/b205892h

second leads to a controlled burn-off of carbon to create the porosity.

There has been much work[7,21,22] studying the pyrolysis of polycarbosilane at temperatures above 1000 °C, but little has been reported on the pyrolysis of PCS at lower temperatures. This paper describes the development and stability of microporosity during the early stages of pyrolysis, up to 700 °C, in both the cross-linked and non-cross-linked polycarbosilane materials, and reports the surface areas, micropore volumes, pyrolysis products and the structural changes found. The stability of the micropores is discussed and comparisons are drawn with analogous pure carbon materials.

2 Experimental

The polycarbosilane used in this study was prepared using a slight modification of the method of Yajima *et al.*,[19] in which 4 wt% of polyborodiphenylsiloxane (ABCR UK Ltd.) was added to polydimethylsilane (Strem UK) and refluxed under flowing nitrogen for 6 h. The product was dissolved in xylene, the solution filtered and the solvent removed. The resulting brown viscous material was then subsequently washed in acetone, producing PCS as a white powder in 50% yield. The material was determined to be PCS by FTIR. Half the material prepared was then cross-linked, by heating in static air, with a ramp rate of 0.16 °C min^{-1} to 200 °C and a dwell time of 1 h.

All pyrolysis experiments were carried out under flowing nitrogen in a Pyrotherm tube furnace controlled by a Eurotherm 818P temperature controller. Approximately 0.7 g of sample was placed in alumina boats and the furnace flushed with oxygen-free nitrogen for 2 h before heating. The samples were heated at 1.66 °C min^{-1} to a range of temperatures between 300 and 700 °C, followed by an isothermal hold for 2.5 h.

BET surface area and pore volume measurements were carried out by nitrogen adsorption at −196 °C using a Beckman Coulter Omnisorp 100cx instrument. All samples were outgassed for 16 h at 175 °C before measurement. CO_2 adsorption measurements were carried out at 0 °C on a sample of the non-cross-linked material.

Fourier transform infrared (FTIR) spectroscopy measurements were made using a Perkin Elmer Paragon 1000 Series machine. Samples of 0.5 to 1.0 mg were mixed with 150 mg of KBr, pressed into 13 mm diameter discs and spectra collected between 400 and 4000 cm^{-1}, with a resolution of 4 cm^{-1}.

Simultaneous thermal analysis (STA), *i.e.* thermogravimetric (TGA) and differential scanning calorimetry (DSC), measurements were made using a Stanton Redcroft STA 625 instrument, aluminium sample pans and an atmosphere of flowing nitrogen (25 cm^3 min^{-1}). Approximately 15 mg of sample was used, with a heating rate of 10 °C min^{-1} to 600 °C.

The use of solid insertion probe mass spectrometry (SIP-MS) in the study of thermal decomposition processes and surface reactions has been described in detail elsewhere.[23] It was used here to study the species evolved during pyrolysis. Essentially, the apparatus consists of a cylindrical microfurnace (12 mm by 5 mm) at the end of a water-cooled stainless steel rod, located in the source of a VG Micromass 7070 high resolution double-focusing mass spectrometer. Temperatures were measured with a type K thermocouple placed at the base of the sample holder. Measurements were made under vacuum (10^{-5} Pa), with a heating rate of 10 °C min^{-1} to 900 °C. Initial mass spectra (mass range 1–300) were taken at 1 s intervals whilst the sample was heated to 800 °C at a rate of 10 °C min^{-1}. The principal evolved gases were identified and their evolution then followed as a function of temperature in subsequent experiments using an MID (multiple ion detector) unit, which employs field switching to give evolved gas profiles for selected species. The m/z = 2 (hydrogen), 16 (methane), 59 (dimethylsilane) and 73 (trimethylsilane) signals were monitored.

The gaseous products of oxidation of material pyrolysed at 550 °C were also studied by evolved gas analysis. Samples were heated at 10 °C min^{-1} to 510 °C in an atmosphere consisting of a mixture of 50% air and 50% He, flowing at 50 cm^3 min^{-1}, and left for 30 min. The O_2 (m/z = 32), CO_2 (44) and H_2O (18) signals were monitored using a Hiden Analytical HPR 20 quadrupole mass spectrometer.

Selected area electron diffraction (SAED) was carried out on powder samples using a Philips CM20 TEM/STEM operated at 200 keV and equipped with a tungsten filament. Areas imaged were also analysed using energy dispersive X-ray (EDX) spectroscopy (Oxford Instruments UTW Light Element EDX detector). The samples pyrolysed at 600 °C were additionally studied in a Philips CM200 Field Emission TEM equipped with a Gatan imaging filter. Samples were prepared by grinding the powders, dispersing them in acetone and placing the dispersion on a holey carbon support film.

MAS-NMR was carried out on selected samples using a Bruker MSL 300 spectrometer equipped with a 7.1 T Oxford Instruments magnet. The ^{29}Si and ^{13}C spectra were acquired at 59.6 and 75.4 MHz, respectively, with the samples ground to a fine powder to facilitate MAS at approximately 3 kHz. Proton decoupling was performed with a radiofreqency field of approximately 40 kHz. 45° Excitation pulses were used to limit saturation. Spectra were processed with 40 Hz of exponential line broadening and chemical shifts referenced to external tetramethylsilane. Cross-polarisation spectra used a spin lock field of approximately 40 kHz.

3 Results and discussion

The FTIR spectra showed that the as-prepared (non-cross-linked) PCS gave rise to characteristic peaks at 2100 (Si–H), and 1350 and 1020 cm^{-1} (Si–CH_2–Si), while the spectrum of the cross-linked PCS did not contain the peak at 2100 cm^{-1}. The molecular weight distribution of the PCS was determined by gel-permeation chromatography (Rapra Technology Ltd.). The M_n was found to be 1400, which compares reasonably well to the M_n value of 1500 quoted for the commercially available Nippon Carbon PCS material. The M_w was 18 000 and the M_w/M_n ratio of 12.8 suggested a broad polymer molecular weight distribution.

TGA plots (to 600 °C) for both the non-cross-linked PCS and the cross-linked material are shown in Fig. 1. The plot for the non-cross-linked material shows two major steps, the first starting at around 125 °C with a weight loss of around 6.5% up to 250 °C, and the second between 325 and 450 °C with a weight loss of approximately 8%. The cross-linked material underwent a weight loss of 3% starting at the higher temperature of *ca.* 325 °C and extending to 525 °C, before a more rapid process commenced at around 550 °C, reflecting the stabilising effects of cross-linking.

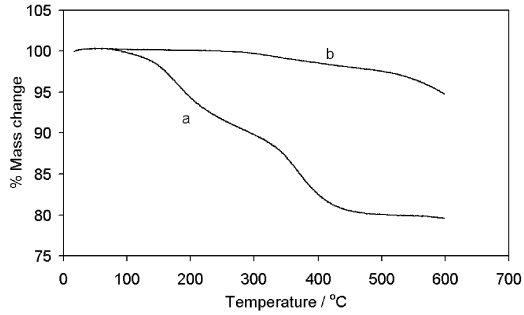

Fig. 1 Thermogravimetric plots for (a) the non-cross-linked and (b) the cross-linked PCS.

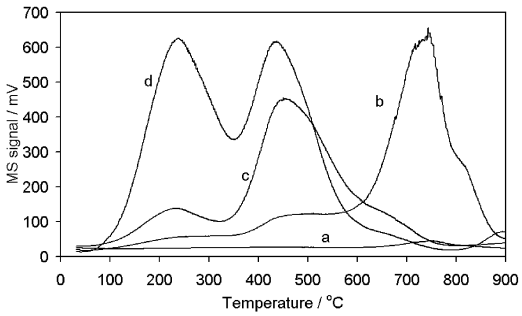

Fig. 2 SIP-MS plot for the non-cross-linked material: (a) hydrogen; (b) methane; (c) dimethylsilane; (d) trimethylsilane.

3.1 Structural evolution during the pyrolysis of PCS

3.1.1 Evolved gas analysis. The SIP-MS data correspond well to the TGA results. The MID unit was set to monitor the four largest signals observed, *i.e.* $m/z = 2$ (hydrogen), 16 (methane), 59 (dimethylsilane) and 73 (trimethylsilane),[22] while the sample was being heated in a vacuum. Fig. 2 shows the evolved gas analysis traces for the non-cross-linked material, with the evolution of species starting at 100 °C being mainly trimethylsilane (plot d) with some dimethylsilane (plot c), while methane (plot b) was also evolved. The trimethylsilane signal reaches a peak at 250 °C, before declining initially and then increasing to a second maximum. The signal for dimethylsilane shows the same trend, but reaches the second maximum at a greater temperature than the trimethylsilane signal (450 °C compared with 425 °C), before decreasing more slowly. These evolved gas analysis signals correspond to the mass losses seen in the TGA measurements. The methane signal rises slowly initially, becoming the dominant peak above 600 °C. Hydrogen (plot a) was evolved at temperatures above 650 °C. The methane signal declines rapidly above 750 °C and reached zero by 900 °C. The species evolved below 550 °C were due to the loss of volatile low molecular weight components of the PCS, while at higher temperatures, the species evolved were due to the polymer to inorganic transition.

Fig. 3 shows the SIP-MS results for the cross-linked PCS. This differs markedly from that of the non-cross-linked material, with no signal seen for trimethylsilane (plot d) below 400 °C and then only a small increase at higher temperatures. The only significant peak is the methane (plot b) signal, starting around 400 °C, before rising rapidly at 600 °C to a maximum at 750 °C prior to declining, but still remaining significant at 900 °C. There is a low broad water signal (plot c) in the range 350 °C to 500 °C corresponding to the small weight loss seen in the TGA results. Hydrogen (plot a) is evolved above 650 °C, reaching a maximum at around 750 °C.

The evolved gas analysis data using SIP-MS for the cross-linked material is consistent with those of Hasegawa.[21] However, our data for the non-cross-linked material differ from those obtained by Bouillon *et al.*[22] and Corriu *et al.*,[24] who both used a commercial PCS, and Hasegawa and Okamura.[6] The latter used a PCS derived from the thermal decomposition of polydimethylsilane in the presence of polyborodiphenylsiloxane as an initiator. The earlier evolved gas analysis measurements conducted by Bouillon *et al.* involved rapidly heating the sample to a set temperature in a mass spectrometer and examining the gases evolved, while Hasegawa simply measured pressure changes due to the evolved gases. Comparisons are difficult due to the differing experimental techniques and sample treatments used. For example, Hasegawa vacuum distilled the PCS at 320 °C, thus removing all volatile components with a boiling point below this temperature, while Bouillon *et al.* only took measurements from 400 °C. Corriu *et al.* saw no evolved species below 370 °C for non-cross-linked PCS using TG-MS, which gave a trace that was similar to the plot obtained for the cross-linked PCS in this study. This suggests that the material they were using had cross-linked or partially cross-linked in their preparation procedure.

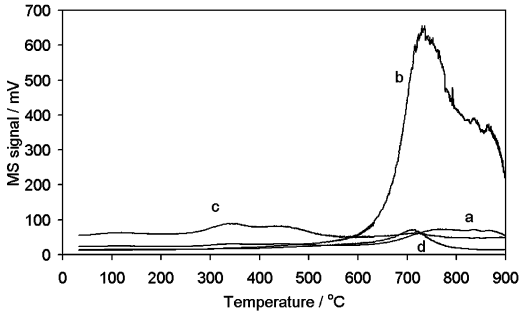

Fig. 3 SIP-MS plot for the cross-linked material: (a) hydrogen; (b) methane; (c) water; (d) trimethylsilane.

He density measurements (Micromeritics Accupyc 330) were carried out on selected samples. The densities increased with increasing pyrolysis temperatures. The starting materials, although non-porous, showed the lowest densities, with that of the cross-linked sample being slighter higher, at 1.35 kg m^{-3}, than the non-cross-linked material, which had a density of 1.16 kg m^{-3}. The samples pyrolysed at 550 °C had similar densities (1.5 kg m^{-3}), which is as expected given that both the cross-linked and non-cross-linked materials were found to have very similar microporosity. The samples pyrolysed at 700 °C had densities graeter than 2 kg m^{-3}.

3.1.2 Solid-state NMR. Fig. 4 shows ^{29}Si MAS NMR spectra for selected samples; assignments are given in the figure. Table 1 lists the expected shifts of a range of species likely to occur in these materials. Note that widely differing species can have similar ^{29}Si chemical shifts, with small additional shifts arising from the exact nature of alkyl groups or through steric effects. Throughout this section, the Si of interest is indicated with an asterisk where more than one Si is included in a species formula. The ^{13}C CP-MAS spectra (not shown) exhibit a broad peak in the region expected for Si–CH_2–Si and Si–CH_3 species, and traces of phenyl resonances.

The non-cross-linked PCS contains a range of species giving rise to strong peaks assigned to Si*C_3(OSi) and SiC_4. In

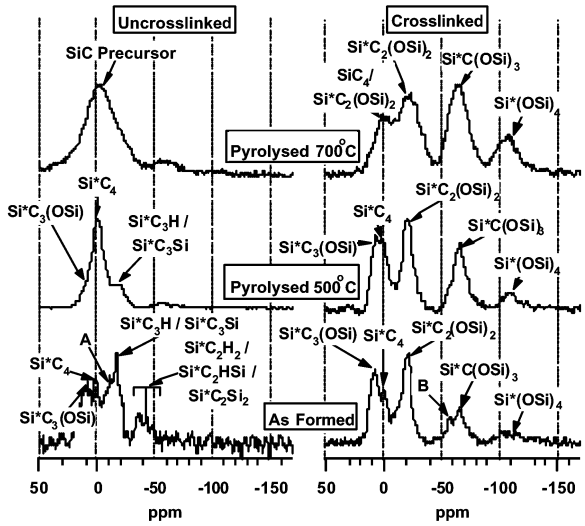

Fig. 4 ^{29}Si MAS NMR spectra of selected samples before and after cross-linking and pyrolysis. Peaks A and B are discussed in the text. Assignments are made on the basis of the data given in Table 1 and the expected species that could be present in these samples.

Table 1 Assignments for polycarbosilanes given in the literature. Note that all shifts are subject to small variations depending on the exact constitutional/steric environment

Species	Expected shift/ppm	Reference
SiC_4	0	6, 25, 26, 29, 31
$SiHC_3$	−17	6, 25, 26, 30
SiH_2C_2	−38	29
SiH_3C	−65 to −69	29
$Si*C_3Si$	−7 to −10	31, 34
$Si*C_2Si_2$	−30 to −38	6, 34
$Si*C_3(OSi)$	10	26
$Si*C_2(OSi)_2$	−20 to −24	27, 28
$Si*C(OSi)_3$	−60 to −67	33
$Si*(OSi)_4$	−110	27

addition, substantial quantities of resonances due to a range of species with Si–Si or Si–H linkages arising from PCS precursors are observed, although since many of these species have similar shifts, exact assignments are uncertain. By analogy to spectra in ref. 30, the broad peak (A) in the range −10 to −15 ppm is probably due to protonated species, but we have been unable to find definitive assignments in the literature. In the long term, ^{13}C–^{29}Si correlation experiments need to be performed to confirm assignments in these and related materials. We estimate an O/Si atomic ratio of approximately 0.2.

On heating the non-cross-linked material to 500 °C, the SiC_4 resonance becomes dominant and the peaks due to PCS precursors largely disappear. Further heating to 700 °C leads to considerable broadening of the peaks, which indicates the presence of a wider or more distorted range of local environments. The spectra are similar to those obtained by other researchers[32] on pyrolysis of polymethylsilane and appear to be due to a silicon carbide precursor phase. Cross-polarisation spectra (not shown) for both ^{13}C and ^{29}Si indicate that most of the hydrogen is removed from the material by the pyrolysis. Thus, the ^{29}Si spectra likely arise from SiC_4 species in a disordered SiC precursor phase where the C atoms are cross-linked to other C or Si species rather than being protonated.

The spectra of the initial PCS sample after cross-linking but before pyrolysis are consistent with the EELS results (section 3.1.3), showing that substantial oxidation has taken place, with significant quantities of highly oxidised species being formed. There is insufficient data in the literature to enable the assignment of the small peak (B) at −57 ppm. On heating the cross-linked material, the changes which take place are relatively straightforward, with the peaks due to non-oxygenated species gradually decreasing in intensity and with the more oxygenated species, such as $Si*(OSi)_4$, becoming more prominent. As with the non-cross-linked material, the line-widths increase, indicating that there is a wider distribution of local environments, consistent with formation of an open disordered structure. Again, CP spectra indicate that nearly all of the hydrogen is removed on pyrolysis to 700 °C, leaving a silicon oxycarbide gel. The predominant species is $Si*C(OSi)_3$, indicating that most of the material exists in a mixed oxycarbide gel rather than as a mixture of SiO_2 or SiC_4 precursor phases.

The various crystalline SiC phases give rise to clear patterns in the NMR spectra in the region 10–25 ppm and do not appear to be formed at all in either system at temperatures up to 700 °C. While relaxation problems can be experienced for SiC phases, all the spectra shown in Fig. 4 were acquired with a 90 s relaxation delay, which should be sufficient to observe qualitative spectra for nearly all SiC samples (see, for example, spectra in ref. 35). There is no evidence for extensive reaction with nitrogen.

In the non-cross-linked material, the Si–Si and Si–H linkages are preferentially lost on pyrolysis, while in the cross-linked material, the more carbonaceous components appear to be preferentially lost. The cross-linked material is substantially more oxygenated prior to pyrolysis.

3.1.3 Electron microscopy. SAED images for the 550 °C pyrolysed non-cross-linked and cross-linked samples showed them to be amorphous, as expected. EDX analysis revealed the presence of silicon, carbon and oxygen in both samples, though with less of the latter in the non-cross-linked sample. The oxygen in the non-cross-linked sample could have come from the processing of the PCS, as polyborodiphenylsiloxane contains oxygen, or the presence of trace amounts of oxygen during pyrolysis.

EELS elemental mapping of the cross-linked PCS material pyrolysed at 550 °C, using the Si $L_{2,3}$-, C K- and O K-edges, showed a reasonably homogeneous distribution of the elements, although a detailed analysis suggested the possibility of some carbon and oxygen enrichment in certain areas (on the sub-nanometer scale), whereas the silicon distribution seemed to be more uniform.

Electron energy-loss spectroscopy (EELS) analysis[36,37] of the cross-linked sample gave a composition of approximately $SiOC_3$ (silicon oxycarbide). The Si $L_{2,3}$ electron loss near edge structure (ELNES) results indicated that both Si–C bonding and Si–O bonding were present, while C K-ELNES suggested both C–C bonding and Si–C bonding. This tends to support the idea of sub-nanometer phase separation in C- and Si–O-rich areas. The non-cross-linked sample pyrolysed at 550 °C had a general composition of approximately Si_3OC_{12}, a silicon oxycarbide, but with much less oxygen than the corresponding cross-linked sample. The shape and position of the Si $L_{2,3}$- and C K-ELNES edges again indicated both Si–C and C–C bonding, with considerably less evidence of Si–O bonding, as might be expected from the lower overall oxygen content of the sample.

Fast Fourier transformation of high resolution images of a thin area recorded at Scherzer defocus provided a power spectrum which was radially averaged using Digital Micrograph software (Gatan).[38] This indicated that the pore structure is located at around 2 and 0.8 nm for the cross-linked sample and at around 1 nm and greater for the non-cross-linked sample.

3.2 Pyrolysis of PCS

After pyrolysis, the powders showed distinct colour changes from colourless to dark brown. The higher the pyrolysis temperature, the darker the colour, with the cross-linked material being darker than the corresponding non-cross-linked material at any given temperature.

The nitrogen adsorption–desorption isotherms (Fig. 5) show the typical Type 1 shape associated with microporous materials. In reporting surface area values, we note that while other workers in this field have quoted BET surface areas, there is doubt about the validity of this equation when applied to microporous materials. We therefore provide BET values for the purposes of comparison only. The more correct micropore

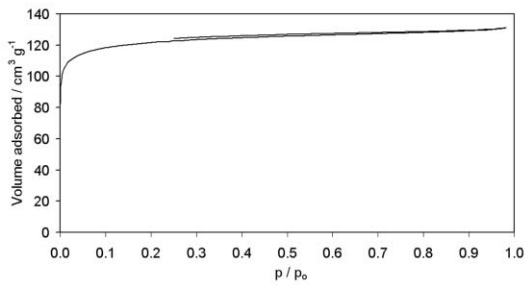

Fig. 5 Type 1 N_2 adsorption–desorption isotherm of a non-cross-linked PCS sample pyrolysed at 600 °C under N_2.

Table 2 Nitrogen adsorption results for the cross-linked and non-cross-linked polycarbosilane

Material	Pyrolysis temp./°C	BET surface area/m^2 g^{-1}	Micropore volume/cm^3 g^{-1}
Cross-linked PCS	300	221	0.12
	400	154	0.10
	500	278	0.14
	550	479	0.21
	600	473	0.20
	700	338	0.16
Non-cross-linked PCS	300	321	0.16
	400	475	0.23
	500	463	0.20
	550	489	0.20
	600	454	0.20
	700	5	0.01

volumes are also given (Table 2). While the cross-linked and non-cross-linked PCS powders showed no porosity or significant surface area, *i.e.* < 0.5 m^2 g^{-1}, prior to pyrolysis, they both developed maximum BET surface areas of around 500 m^2 g^{-1}. However, the non-cross-linked material exhibited a plateau of maximum surface area between the pyrolysis temperatures of 400 to 600 °C, before falling to less than 5 m^2 g^{-1} at 700 °C, while that of the cross-linked material rose to a maximum at higher temperatures (550–600 °C) before decreasing more slowly on further heating. The maximum micropore volumes obtained were in the region of 0.2 cm^3 g^{-1} for both the cross-linked and non-cross-linked materials, values which are less than those found in commercial activated carbons (typically in excess of 0.3 cm^3 g^{-1}). The micropore volumes were calculated using the model of Dubinin and Astakhov, choosing the most appropriate exponent.[39]

The BET surface area results for the cross-linked PCS sample compare well with the values obtained by Li *et al.*,[8] who used a cross-linked commercial source of the same material and found a maximum apparent surface area of 500 m^2 g^{-1} at a pyrolysis temperature of 550 °C. The slightly lower temperature found for the maximum surface area in that work is probably due to differences in the polycarbosilane starting materials. Using non-cross-linked PCS, Dismukes *et al.*[13] also found that the maximum BET surface area occurred at a pyrolysis temperature of 550 °C, but the maximum BET surface area reported was slightly higher, at 550 m^2 g^{-1}, while the micropore volume was 0.17 cm^3 g^{-1}.

Adsorption of CO_2 at 0 °C and pressures up to 1 atm is confined mainly to the so-called 'ultra-micropores'.[40] Thus, comparison of the micropore volumes determined by CO_2 adsorption and the Dubinin–Astakhov method can provide additional information about the micropore structure. In order to determine whether the micropores were closing up as the pyrolysis temperature was increased, a CO_2 adsorption isotherm was measured for the 700 °C pyrolysed non-cross-linked sample. The nitrogen adsorption results suggest that there are no micropores present (a micropore volume of 0.01 cm^3 g^{-1}), while the CO_2 data shows a micropore volume of 0.09 cm^3 g^{-1}. It is clear that although the pores are closing in this heat treatment temperature region, as shown by the N_2 data, they are not yet fully inaccessible, but the pore openings are extremely small (*i.e.* $<$ *ca.* 0.5–0.6 nm).

3.3 Stability of porosity

The stability of the microporous structure was checked using nitrogen adsorption measurements after 6 months storage in air and no changes were seen in surface area and pore volume. Further work is required to check the long term stability of the microporosity under inert or reducing atmospheres at elevated temperatures, but preliminary studies indicate no rapid losses in the short term.

The oxidative stability of the materials pyrolysed at 600 °C

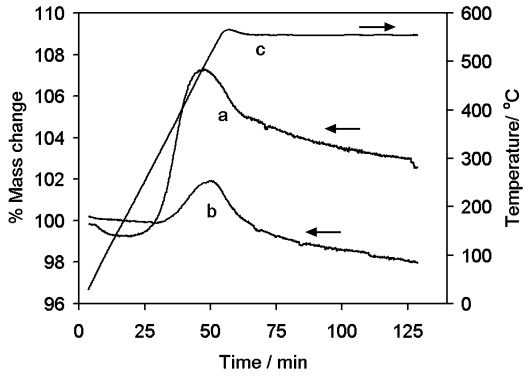

Fig. 6 TG plots against time using a ramp of 10 °C min^{-1} to 550 °C and a 75 min dwell in static air for (a) the non-cross-linked sample and (b) the cross-linked sample. Trace c is a plot of the sample temperature against time.

was examined using TGA in static air, heating at 10 °C min^{-1} with a 75 min dwell at 550 °C for both the cross-linked and non-cross-linked samples (Fig. 6). The plots are broadly similar, but show some significant differences. The non-cross-linked material (trace a) shows a weight increase of 7% starting at 280 °C and rising to a maximum at 490 °C, before falling by 2% at 550 °C and a further 3% after the 75 min dwell time. The material was colourless after this treatment. The cross-linked material (trace b) underwent a significantly lower weight gain of 2%, starting at a higher temperature (350 °C) and reaching a maximum at around 520 °C, followed by a steady weight loss of 4% after 75 min at 550 °C. There was no noticeable change in the dark brown colour of the sample at the end of the run. The initial weight increases suggest that both materials initially adsorb oxygen and that this is followed by a weight loss due to the burning off of carbon.

The PCS samples pyrolysed at 700 °C were also studied by TGA in static air. Neither the cross-linked nor non-cross-linked samples showed any colour change. The TGA plots were similar to the respective plots of the 550 °C pyrolysed samples, with similar mass gains, although they did not show the weight loss seen with those samples during the dwell period. It is known[41] that Nicalon fibres produced from a similar precursor are oxidation resistant and, presumably, the structural changes that lead to this behavior begin around 700 °C.

After subsequent heating in air at 550 °C for 1 h of both the cross-linked and non-cross-linked polycarbosilane materials pyrolysed at 600 °C, the apparent surface area (N_2 adsorption) fell to less than 1 m^2 g^{-1}, showing that the structure is not stable in air at such elevated temperatures. However, CO_2 adsorption measurements, at 0 °C, on the non-cross-linked sample after air treatment at 550 °C gave a micropore volume of 0.02 cm^3 g^{-1}. This result suggests some porosity is still present in the sample but that it is inaccessible to N_2 molecules at 77 K.

The evolved gas analysis plots, in an oxidising atmosphere (a mixture of 50% air and 50% He, flowing at 50 cm^3 min^{-1}) for the PCS samples which had been previously pyrolysed at 550 °C are shown for the cross-linked material in Fig. 7 and for the non-cross-linked material in Fig. 8. The plot for cross-linked sample shows that at around 300 °C the CO_2 (trace c) and H_2O (trace a) signals start to rise, while the O_2 (trace b) signal falls dramatically. The maximum in the CO_2 signal is seen at around 425 °C and the peak is fairly broad. The maximum O_2 consumption occurs at *ca.* 450 °C. The water signal is very broad, extending from 350 up to 510 °C. The non-cross-linked material differs from the cross-linked material in that the signals start to change at around 200 °C and the water signal does not increase significantly. The minimum in the O_2 (trace b) signal occurs at around 300 °C, while the maximum in

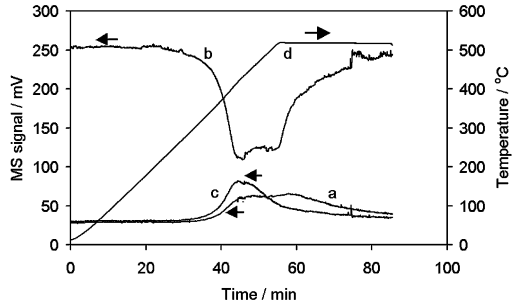

Fig. 7 Evolved gas analysis of cross-linked PCS, previously pyrolysed at 550 °C, heated at 10 °C min^{-1} to 510 °C with a 30 min dwell under a mixture of flowing 50% air and 50% He (50 cm^3 min^{-1}): (a) H_2O; (b) O_2; (c) CO_2. Trace d is a plot of the sample temperature against time.

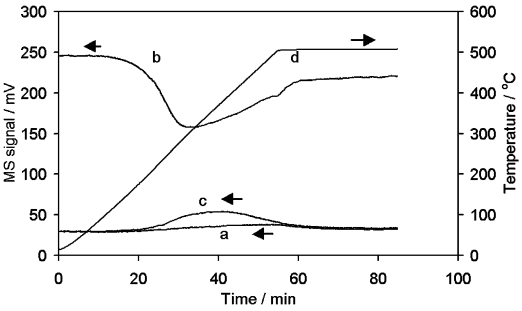

Fig. 8 Evolved gas analysis of non-cross-linked PCS, previously pyrolysed at 550 °C, heated at 10 °C min^{-1} to 510 °C with a 30 min dwell under a mixture of flowing 50% air and 50% He (50 cm^3 min^{-1}): (a) H_2O; (b) O_2; (c) CO_2. Trace d is a plot of the sample temperature against time.

the CO_2 (trace c) signal is found at a higher temperature of around 350 °C, and the peak is much broader than for the cross-linked material. The fall in the O_2 signal corresponds to the increase in mass of both the cross-linked and non-cross-linked samples seen in the TG plots due to oxygen uptake, the rate of which is greater than the rate of carbon burn-off.

The burn-off of carbon from these samples was accompanied by loss of micropore volume. Samples of the pyrolysed (550 °C) cross-linked and non-cross-linked PCS were heated for 30 min in an oxidising atmosphere (static air) at various temperatures up to 510 °C and their micropore volumes measured by nitrogen adsorption (Fig. 9). The cross-linked sample could be heated to 230 °C before the micropore volume started to fall, while the non-cross-linked sample could only be heated to 130 °C before the micropore volume started to decrease, reaching zero at 460 °C. However, at 130 °C, the cross-linked sample still contained some micropores.

A sample of the above pyrolysed cross-linked PCS was heated at 250 °C for 1 h under flowing steam, a mild oxidant, in a nitrogen carrier gas, which resulted in no change in the micropore volume. However, when the non-cross-linked material was heated at 200 °C for 1 h in steam, the micropore volume fell to 0.16 cm^3 g^{-1}. These results confirm the observations from the STA measurements that the material derived from the cross-linked PCS is more resistant to oxidation than the non-cross-linked material.

The lack of stability of the micropore structure in oxidising gases means that the use of these materials is limited to either reducing atmospheres or processes where low temperatures are required. Fortunately, the main areas of application of most membrane reactors require a strongly reducing atmosphere.

The development of microporosity in these materials occurs with the loss of volatile components during pyrolysis. This

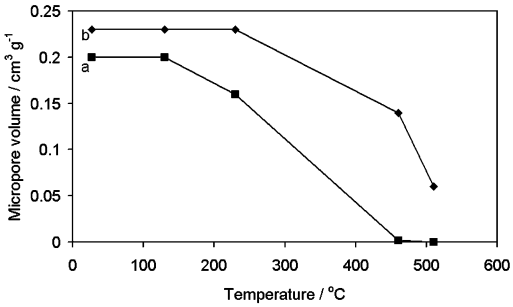

Fig. 9 Plot of micropore volume against temperature for (a) non-cross-linked and (b) cross-linked PCS samples, previously pyrolysed at 550 °C, heated under static air for 30 min at each temperature.

accounts for the differences in micropore volumes between the cross-linked and non-cross-linked material, as the SIP-MS results show that material is evolved at much lower temperatures in the non-cross-linked PCS compared to the cross-linked sample. The details of the mechanism of formation of the microporosity in the PCS-derived materials are not known. The microporous materials have been found to be amorphous, but with evidence from the electron microscopy that, on a sub-nanometer scale, a separate carbon-rich phase is present. It may be surmised that the pores are formed in carbon-rich microareas, as this would account for the loss of porosity on heating to 500 °C in air. The 550 °C pyrolysed materials have an open microporous structure, which means that oxygen has ready access to the carbon. This contrasts with commercial Nicalon SiC fibres, which are pyrolysed at 1200 °C and which are relatively stable in air, suggesting that the carbon is inaccessible to oxygen.

The fact that the maximum apparent surface areas and pore volumes are similar for both the cross-linked and non-cross-linked polycarbosilane materials suggests that the amount of material available to form the microporosity is similar for both materials despite the significant loss of mass in the non-cross-linked materials during pyrolysis. The loss of the microporosity at pyrolysis temperatures above 700 °C is caused by the structural rearrangements that occur during the pyrolysis process in which methane and hydrogen are lost and the PCS changes from a polymer to an amorphous inorganic material.

4 Conclusions

The pyrolysis, to 700 °C, of both cross-linked and non-cross-linked polycarbosilane resulted in the development of microporous materials, the maximum apparent surface areas and pore volumes for both materials being similar. However, differences occurred, with the non-cross-linked material having a plateau region of highest surface areas between 400 and 600 °C, while that of the cross-linked material rose to a maximum at around 600 °C. A further difference in the two materials is that at 700 °C, the microporosity revealed by N_2 adsorption measrements was lost in the non-cross-linked material, but was still apparent in the cross-linked material. The non-cross-linked material evolved volatile species above 100 °C, which may contribute to the early development of the plateau region seen in the plot of surface area against pyrolysis temperature. These volatile species were not evolved from the cross-linked material and so contributed less to the development of microporosity at the lower pyrolysis temperatures. The loss of microporosity at 700 °C for the non-cross-linked sample arose from the conversion from a polymer to an amorphous inorganic material and occurred at a lower temperature than in the cross-linked sample, the maximum microporosity occurring at the point where this transition began.

These materials show similar behavior to microporous carbons. Electron microscopy provided evidence for some phase separation, on a sub-nanometer scale, of carbon-rich areas, in which the micropores might be located.

The micropores have been found to be stable in air at room temperature for extended periods, but were not stable in oxidising atmospheres at elevated temperatures for both cross-linked and non-cross-linked samples, although the former was found to be more resistant to oxidation. This limits the high temperature application of these materials to inert and reducing atmospheres only. The reduction of porosity in oxidising atmospheres at high temperatures is consistent with the suggestion that the pores are located in carbon-rich areas.

Acknowledgement

The work was supported by the EPSRC through the ROPA programme, grant no. GR/L74064.

References

1 S. Yajima, J. Hayashi, M. Omori and K. Okamura, *Nature (London)*, 1976, **261**, 683–685.
2 S. Yajima, M. Omori, J. Hayashi, K. Okamura, T. Matsuzawa and C. Liaw, *Chem. Lett.*, 1976, 551.
3 P. Colombo, T. E. Paulson and C. G. Pantano, *J. Am. Ceram. Soc.*, 1997, **80**, 2333–2340.
4 K. Langguth, S. Bockle, E. Muller and G. Roewer, *J. Mater. Sci.*, 1995, **30**, 5973–5978.
5 O. Delverdier, M. Monthioux, D. Mocaer and R. Pailler, *J. Eur. Ceram. Soc.*, 1993, **12**, 27–41.
6 Y. Hasegawa and K. Okamura, *J. Mater. Sci.*, 1983, **18**, 3633–3648.
7 E. Bouillon, D. Mocaer, J. F. Villeneuve, R. Pailler, R. Naslain, M. Monthioux, A. Oberlin, C. Guimon and G. Pfister, *J. Mater. Sci.*, 1991, **26**, 1517–1530.
8 Z. Li, K. Kusakabe and S. Morooka, *J. Membr. Sci.*, 1996, **118**, 159–178.
9 K. Kusakabe, Z. Li, H. Maeda and S. Morooka, *J. Membr. Sci.*, 1995, **103**, 175–180.
10 K. Kusakabe, Z. Li, H. Maeda and S. Morooka, *Sep. Sci. Technol.*, 1997, **32**, 1233–1254.
11 A. B. Shelekhin, E. J. Grosgogeat and S. Hwang, *J. Membr. Sci.*, 1991, **66**, 129–141.
12 E. J. Grosgogeat, J. R. Fried, R. G. Jenkins and S. Hwang, *J. Membr. Sci.*, 1991, **57**, 237–255.
13 J. P. Dismukes, J. W. Johnson, J. L. Pizzulli and R. A. McEvoy, *Proc. Electrochem. Soc.*, 1999, **97–98**, 196.
14 J. P. Dismukes, J. W. Johnson, J. S. Bradley and J. M. Miller, *Chem. Mater.*, 1997, **9**, 699–706.
15 J. Zaman and A. Chakma, *J. Membr. Sci.*, 1994, **92**, 1–28.
16 G. Saracco, G. F. Versteeg and W. P. M. Van Swaaij, *J. Membr. Sci.*, 1994, **95**, 105–123.
17 S. Yajima, Y. Hasegawa, J. Hayashi and M. Omori, *J. Mater. Sci.*, 1978, **13**, 2569.
18 R. M. Laine and F. Babonneau, *Chem. Mater.*, 1993, **5**, 260–279.
19 S. Yajima, Y. Hasegawa, K. Okamura and T. Matsuzawa, *Nature (London)*, 1978, **273**, 525–527.
20 T. Ishikawa, M. Shibuya and T. Yamamura, *J. Mater. Sci.*, 1990, **2**, 2809–2814.
21 Y. Hasegawa, *J. Mater. Sci.*, 1989, **24**, 1177–1190.
22 E. Bouillon, F. Langlais, R. Pailler, R. Naslain, F. Cruege, P. V. Hong, J. C. Sarthou, A. Delpuech, M. Monthioux and A. Oberlin, *J. Mater. Sci.*, 1991, **26**, 1333–1345.
23 P. A. Barnes, G. M. Parkes and P. Sheridan, *J. Therm. Anal.*, 1994, **42**, 841–854.
24 R. J. P. Corriu, D. Leclercq, P. H. Mutin and A. Vioux, *Chem. Mater.*, 1992, **4**, 711–716.
25 T. Taki, M. Inui, K. Okamura and M. Sato, *J. Mater Sci. Lett.*, 1989, **8**, 918–920.
26 R. K. Harris, *J. Magn. Reson.*, 1975, **17**, 174.
27 J. Brus and J. Dybal, *Polymer*, 2000, **41**, 5269–5282.
28 G. J. J. Out, A. A. Turetskii, M. Mollerand and D. Oelfin, *Macromolecules*, 1994, **27**, 3310–3318.
29 C. K. Whitmarsh and L. V. Interrante, *J. Organomet. Chem.*, 1991, **1**, 69–77.
30 Y. Hasegawa and K. Okamura, *J. Mater. Sci.*, 1986, **21**, 321–328.
31 A. E. Aliev, K. D. M. Harris and D. C. Apperley, *J. Chem. Soc., Chem. Commun.*, 1993, 251–253.
32 Z.-F. Zhang, F. Babonneau, R. M. Laine, Y. Mu, J. F. Harrod and J. A. Rahn, *J. Am. Chem. Soc.*, 1991, **74**, 670–673.
33 M. P. Besland, C. Guizard, H. Hovnaian, A. Larbot, L. Cot, J. Sanz, I. Sobrados and M. Gregorkiewitz, *J. Am. Chem. Soc.*, 1991, **113**, 1982–1987.
34 M. F. Gozzi and I. V. P. Yoshida, *Macromolecules*, 1995, **28**, 7235–7240.
35 J. S. Hartman, M. F. Richardson, B. L. Sherriff and B. G. Winsborrow, *J. Am. Chem. Soc.*, 1987, **109**, 6059–6067.
36 X. X. Jiang, R. Brydson, S. P. Appleyard and B. Rand, *J. Microsc.*, 1999, **196**, 203–212.
37 D. Upadhaya, R. Brydson, C. M. Wardclose, P. Tsakiropoulos and F. H. Froes, *Mater. Sci. Technol.*, 1994, **10**, 797–806.
38 K. Oshida, K. Kogiso, K. Matsubayashi, K. Takeuchi, S. Kobayashi, M. Endo, M. S. Dresselhaus and G. Dresselhaus, *J. Mater. Res.*, 1995, **10**, 2507–2517.
39 S. J. Gregg and K. S. W. Sing, *Adsorption, Surface Area and Porosity*, Academic Press, London, 1984, p. 226.
40 D. Cazorla-Amoros, J. Alcaniz-Monge and A. Linares-Solano, *Langmuir*, 1996, **12**, 2820–2824.
41 T. Shimoo, H. Chen and K. Okamura, *J. Mater. Sci.*, 1994, **29**, 456–463.